ELSEVIER

Polymer Vol. 37 No. 13, pp. 2641–2651, 1996

0032-3861/96/$15.00+0.00

Micromechanical transitions in compatibilized polymer blends

H. Eklind and F. H. J. Maurer*
Department of Polymer Technology, Chalmers University of Technology, S-41296 Göteborg, Sweden
(Received 2 May 1995)

The viscoelastic properties of compatibilized poly(2,6-dimethyl-*p*-phenylene oxide) and poly(methyl methacrylate) (PPO/PMMA) blends were studied by dynamic mechanical spectroscopy (d.m.s.) and the experimental data compared with an interlayer model. An interphase created by a poly(styrene-*graft*-ethylene oxide) (P(S-*g*-EO)) copolymer was found to significantly affect the dynamic mechanical behaviour of these blends, and it is shown that the addition of the copolymer results in a new transition in the blends. This is theoretically shown to be a 'micromechanical transition', and is explained by the change in relative moduli values of the components in the matrix–interphase–particle structure of the blends, and not to originate from a molecular transition in any of the constituents. The micromechanical transition temperature is predicted to depend on the volume fraction and the Poisson ratio of the interphase and is affected by the influence of PPO and PMMA on the properties of the interphase. Copyright © 1996 Elsevier Science Ltd.

(Keywords: dynamic mechanical spectroscopy; interphase; micromechanical transition)

INTRODUCTION

Polymer blending is a useful technique for designing materials with a wide variety of properties. An important commercial advantage is that polymer blends offer a way to produce new materials by using already existing materials, which thus reduces development costs. However, as most polymer blends are immiscible and form heterogeneous multiphase systems, blending often results in material properties that are strongly dependent on the processing conditions, morphology and interactions between the phases. Numerous examples in the literature[1–6] show that the addition of a small amount of a 'compatibilizer', i.e. a block or graft copolymer which interacts favourably with both major constituents, to an immiscible binary blend may enlarge the interfacial area owing to a decrease in interfacial tension. This will result in a finer and more processing-insensitive morphology. The interfacial tension is decreased because the compatibilizer forms an 'interphase' between the immiscible phases. As an interphase is considered to have a certain volume with its own characteristic properties or property gradients, and as most blends are subjected to external forces during preparation and application, the effect of the interphase in multiphase polymer blends on the viscoelastic properties is of great importance.

In this present paper, the effect of an interphase created by the addition of a graft copolymer on the viscoelastic properties of an immiscible blend is studied experimentally by dynamic mechanical spectroscopy (d.m.s.). The experimental dynamic mechanical data are compared with an interlayer model derived by Maurer[7,8], which allows the prediction of the viscoelastic properties of immiscible polymer blends which include an interphase in the melt and solid state from the complex properties of the pure constituents, without the use of any fitting parameters. This interlayer model is an extension of the spherical-shell model of van der Poel[9], as corrected by Schwarzl and van der Eikhoff[10] and Smith[11]. Originally, van der Poel derived a model for the viscosity and shear modulus for elastic and particulate-filled systems without an interphase, and this model was later extended to include viscoelastic species with an interphase for the description of shear modulus[7], bulk modulus[7,12] and thermal expansivity[8,12,13]. An analogous procedure was followed to derive the complex dielectric properties[8,14,15] for composites and blends with interphases. The primary assumptions for calculating the shear modulus are non-interacting spherical inclusions in the matrix, homogeneous and isotropic components, continuity of displacements, radial and tangential stresses at the boundaries of the phases, insignificant inertial forces, the absence of defects and no thermal stresses.

Recently, much attention has been given to the experimental and theoretical effects of interfacial tension on the dynamic mechanical properties of immiscible polymer melts at low frequencies[16–20]. We have primarily studied the blends in the solid state, where this effect is negligible. The interlayer model we used does not take into account the effect of interfacial tension. The interlayer model has been shown to accurately describe the viscoelastic response of polymers filled with high-moduli isotropic particles[21], even when an interphase is present[7]. We have also previously[22] applied the model for two immiscible binary systems, i.e. PS/PEO and

* To whom correspondence should be addressed

PS/PMMA, in which the effect of an interphase is considered to be negligible.

The experimental ternary system studied in this work consists of poly(2,6-dimethyl-*p*-phenylene oxide) (PPO) and poly(methyl methacrylate) (PMMA) homopolymers, with the addition of a graft copolymer with polystyrene (PS) backbones and poly(ethylene oxide) (PEO) side chains (P(S-*g*-EO)). PPO and PMMA are immiscible and form a two-phase system[23]. In a previous paper[24], we studied the effect of the copolymer on the mobility, miscibility and morphology of binary and ternary blends of PPO, PMMA and P(S-*g*-EO). Experimental d.m.s. data showed only one T_g in the binary PPO/P(S-*g*-EO) and PMMA/P(S-*g*-EO) blends, at slightly lower temperatures than the T_g values of the homopolymers. Room-temperature nuclear magnetic resonance (n.m.r.) spectra showed that the relaxation times of the PEO side chains were approximately the same in PMMA/PEO and PMMA/P(S-*g*-EO) blends, while the relaxation times of PEO in PPO/P(S-*g*-EO) blends were quite different from both PPO and the pure copolymer. These experiments indicated that the PEO side chains of the copolymer were at least partially miscible on a microscopic length-scale with PMMA. On the other hand, the PEO side chains did not seem to be miscible with PPO, although only one T_g could be observed in the blends. This suggested that the PS backbone of the copolymer was at least partially miscible with PPO. These experiments implied that the copolymer acts as a compatibilizer in the PPO/PMMA system, and this was verified by scanning electron microscopy (SEM), which showed that the addition of P(S-*g*-EO) to a PPO/PMMA blend reduced the dispersed phase size.

The aim of this present paper is to ascertain whether it is possible to use the interlayer model for compatibilized blends in general, where the effect of the interphase properties and volume fraction is not negligible, and to study the influence of different viscoelastic properties of the interphase on the dynamic mechanical response in the specific PPO/PMMA/P(S-*g*-EO) system. It will be shown both experimentally and theoretically that the specific viscoelastic characteristics of the constituents can give rise to a 'micromechanical transition' in the blends, which is not present in any of the constituents when an interphase with its own characteristic properties is present. The frequency and temperature dependence of the molecular and micromechanical transitions in the PPO/PMMA/P(S-*g*-EO) system are presented in a separate paper[25].

THEORETICAL CONSIDERATIONS

Rheological definitions

The rheological parameter used in the theoretical calculations is the complex shear modulus, $G^*(\omega, T)$, which is defined as follows:

$$\begin{aligned} G^*(\omega, T) &= G'(\omega, T) + iG''(\omega, T) \\ &= G_d(\omega, T)\exp(i\delta(\omega, T)) \end{aligned} \quad (1)$$

$G'(\omega, T)$ and $G''(\omega, T)$ are the shear storage and shear loss modulus, respectively, which are determined from the experimentally measured dynamic shear modulus, $G_d(\omega, T)$, and phase angle, $\delta(\omega, T)$. $G_d(\omega, T)$ is defined as the quotient of the amplitude of the sinusoidal stress and the sinusoidal strain, while $\delta(\omega, T)$ is defined as the phase angle between the strain (input) and the stress (output). Both quantities are measured at specific angular frequencies, ω, and temperatures, T. In the following text, the indices b, m, i and p correspond to the blend, matrix, interphase and particle phases, respectively.

Modelling

An interlayer model with an interphase[7,8] was used to predict the dynamic mechanical shear properties of the blends for comparison with the experimental results. We repeat here the basic equations for this model.

Consider a model of a polymer blend with spherical particles of one phase included in a matrix of another phase and with an interphase between the particles and the matrix. The major feature of this model is that a representative volume element (RVE) with the shape of a cube, containing one spherical particle surrounded by a shell of interphase, which in turn is covered by a shell of matrix material, and which finally is surrounded by blend material, is subjected to an external shear stress field. The RVE as described above is depicted in *Figure 1a*. The radii of the shells are chosen corresponding to the volume fractions of the spherical particles (Φ_p), interphase (Φ_i) and matrix (Φ_m), as follows:

$$\Phi_p = a^3; \qquad \Phi_i = b^3 - a^3; \qquad \Phi_m = 1 - b^3 \quad (2)$$

According to the model, there is pure interphase material in the immediate vicinity of a spherical particle, and somewhat further away there is pure matrix material. Even further away, however, are the properties described by the overall blend material. This RVE is assumed to respond to external stresses as a cube of the blend material. To calculate the dynamic shear modulus of the model blend, the cubic RVE is subjected to a dilatation-free and rotationally symmetrical stress field in the x-, y-, and z-directions according to equations (3)–(5). The directions and angles used in the discussion are defined in *Figure 1b*.

$$\sigma_x = \sigma_y = -\sigma \quad (3)$$

$$\sigma_z = 2\sigma \quad (4)$$

$$\sigma_{xy} = \sigma_{yz} = \sigma_{xz} = 0 \quad (5)$$

The result of this stress field is that both the mean normal stresses and the dilatation are zero. The external stresses are written in polar coordinates as follows:

$$\sigma_{rr} = 2\sigma\tfrac{1}{2}(3\cos^2\theta - 1) \quad (6)$$

$$\sigma_{r\theta} = \sigma(-3\cos\theta\sin\theta) \quad (7)$$

$$\sigma_{r\varphi} = 0 \quad (8)$$

Using Hooke's law and the stress–displacement relationships[26], the displacements u, v and w in the r, θ and φ directions, respectively, can be expressed according to equations (9)–(11), as follows:

$$u = \frac{\sigma r}{G}\tfrac{1}{2}(3\cos^2\theta - 1) \quad (9)$$

$$v = \frac{\sigma r}{2G}(-3\cos\theta\sin\theta) \quad (10)$$

$$w = 0 \quad (11)$$

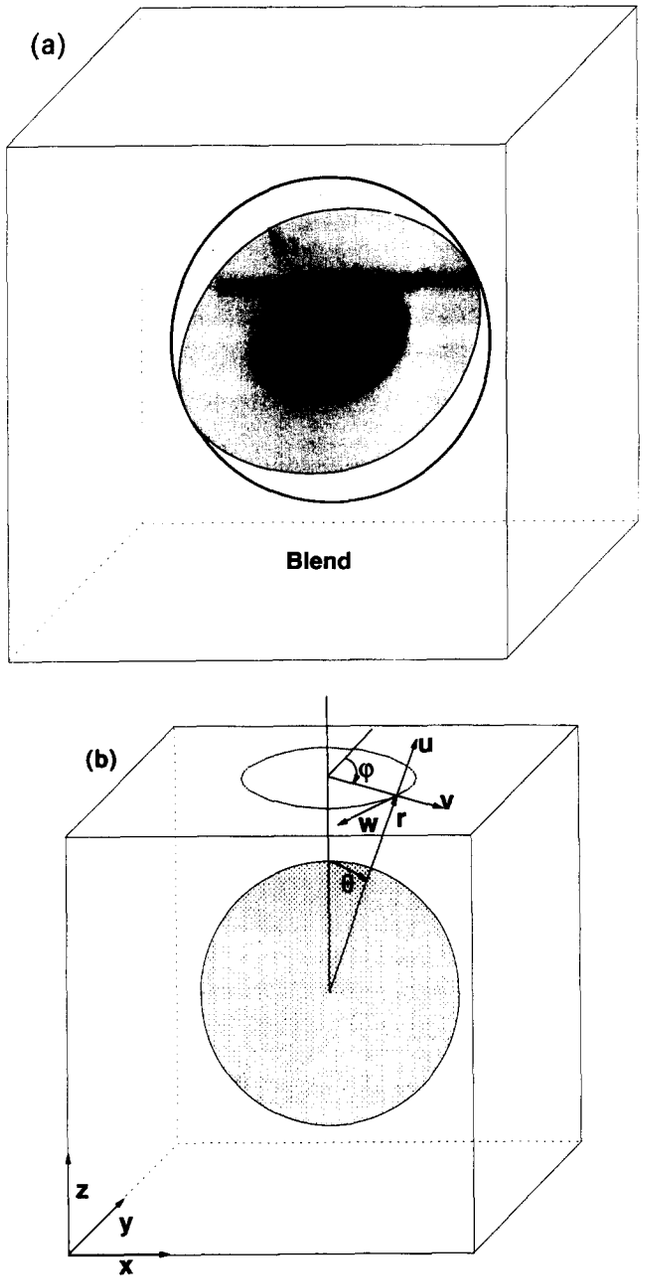

Figure 1 (a) A representative volume element of the interlayer model. (b) Definitions of the x-, y-, z-, u-, v-, w-, and r-directions and the θ and φ angles in the representative volume element

This stress field is rotationally symmetric, and the common solutions to these equations are derived elsewhere[10,11,26] and given as follows:

$$u = (Ar + Br^{-4} + Cr^3 + Dr^{-2})\tfrac{1}{2}(3\cos^2\theta - 1) \quad (12)$$

$$v = (\tfrac{1}{2}Ar - \tfrac{1}{3}Br^{-4} + pCr^3 + qDr^{-2})(-3\cos\theta\sin\theta) \quad (13)$$

$$\text{where } p = \frac{7-4\nu}{12\nu}; \qquad q = \frac{1-2\nu}{5-4\nu} \quad (14)$$

In the above ν represents the Poisson ratio. The radial and tangential stresses are then given as follows:

$$\sigma_{rr} = 2G(A - 4Br^{-5} + k_1Cr^2 + k_3Dr^{-3})\tfrac{1}{2}(3\cos^2\theta - 1) \quad (15)$$

$$\sigma_{r\theta} = G(A + \tfrac{8}{3}Br^{-5} + k_2Cr^2 + k_4Dr^{-3})(-3\cos\theta\sin\theta) \quad (16)$$

$$\text{where } k_1 = -\tfrac{1}{2}; \qquad k_2 = \frac{7+2\nu}{6\nu}; \qquad k_3 = -\frac{2(5-\nu)}{5-4\nu}; \qquad k_4 = \frac{2(1+\nu)}{5-4\nu} \quad (17)$$

The above equations for the displacements and the stresses are valid for the matrix, interphase and particle phase, as well as for the blend, with the specific constants A, B, C and D for each component, respectively. The boundary conditions for the disposition of the equation system for calculating the dynamic shear modulus of the blend are:

(1) For $r = a$, $r = b$ and $r = 1$, the displacements and the radial and the tangential stresses must be continuous. Using equations (12), (13), (15) and (16), this continuity condition gives a system of 12 equations. As each component of the model gives 4 unknown constants (a total of 16 constants), this means that 4 constants must be determined before the equation system can be solved.
(2) For $r = 0$, the displacements in the particles are finite. Equations (12) and (13) can then only be fulfilled if $B_p = D_p = 0$.
(3) For $r \gg 1$, the stresses in the blend must also be finite. This means that equations (15) and (16) are fulfilled only if $C_b = 0$.

The dilatation, e, of the blend then becomes:

$$e = -\frac{(1-2\nu_b)}{(5-4\nu_b)}\frac{3}{2}D_b r^{-3}(3\cos 2\theta + 2) \quad (18)$$

In equation (18), the dilatation already goes to zero for small values of r. If D_b is set to zero in order to force the dilatation of every r-value in the blend material to be zero, the influence of the stresses on the blend material is restricted to higher magnitudes of $1/r$. With these boundary conditions, the general expressions for the displacements and stresses in a rotationally symmetrical stress field lead to a set of 12 linear equations. To obtain a non-trivial solution to the problem, the determinant of the coefficients should vanish. Because of the dimension of the calculations, it is almost impossible to determine an analytical expression for G_b. By matrix manipulation, the determinant can be split into a number of sub-determinants so that G_b is separated. This reduction of the determinant can be evolved into a quadratic equation as regards G_b, which makes it possible to predict the elastic shear modulus of the blend without the use of any fitting parameters, by assuming purely elastic properties of the materials. The description also includes the Einstein solution[27] for hard spheres in an incompressible matrix and infinite dilution. By using the correspondence principle[28], the model can be extended to predict the viscoelastic properties of a blend from the complex properties and the volume fractions of the pure constituents, by assuming linear viscoelastic properties of both the constituents and the blend. The quadratic equation with the complex properties is given in equation (19), as follows:

$$40|\alpha|\left[\frac{G_b^*(\omega,T)}{G_m^*(\omega,T)}\right]^2 + (2|\beta| + 8|\gamma|)\left[\frac{G_b^*(\omega,T)}{G_m^*(\omega,T)}\right] - 5|\tau| = 0 \quad (19)$$

$G_b^*(\omega, T)$ and $G_m^*(\omega, T)$ represent the complex shear modulus of the blend and matrix, respectively, while $|\alpha|$, $|\beta|$, $|\gamma|$ and $|\tau|$ are tenth order determinants with coefficients that are functions of the shear moduli, Poisson ratios and volume fractions of the matrix, interphase and particle phase. The elements of the determinants are presented in the Appendix.

Calculations of the theoretical response of the blends, i.e. $G_b^*(\omega, T)$, at certain angular frequencies and temperatures are performed by using a computer program. The input data needed are the volume fractions, Poisson ratios and the complex shear moduli of the matrix, interphase and particle phase under the same conditions. The major homopolymer component in the experiments was chosen as the matrix phase, while the minor homopolymer component was chosen as the spherical particle phase. The input data for the interphase was chosen by using both original and modified experimental copolymer data, as presented in the Results section.

EXPERIMENTAL

Materials

The PPO and PMMA homopolymers used in this study were both obtained from Scientific Polymer Products, Inc. PPO had a $\bar{M}_w$ of 50 kg mol^{-1} and a density of 1060 kg m^{-3}, while PMMA had a $\bar{M}_w$ of 75 kg mol^{-1} and a density of 1200 kg m^{-3}, according to the manufacturer. The PS–PEO graft copolymer, designated 'P(S-*g*-EO)', was prepared by ethoxylation of an amide-containing styrene copolymer. The backbone of the copolymer was first synthesized by a free-radical reaction with styrene and acrylamide, after which the amide groups were used as initiator sites for the polymerization of ethylene oxide. The backbone contained 5 mol% acrylamide and the total graft copolymer contained 39 wt% PEO. The number-average molecular masses of the backbone and side chains were determined by size exclusion chromatography (s.e.c.) to be 80 and 1.3 kg mol^{-1}, respectively. Details of the preparation and characterization of P(S-*g*-EO) have been described previously[24,29].

Sample preparation

Binary and ternary blends containing PPO, PMMA and P(S-*g*-EO) were prepared in the melt state in a Brabender AEV 330. Blends of PPO and PMMA, with a common composition of 30 volume parts of PPO and 70 volume parts of PMMA, were prepared with additional amounts of 0, 1, 2, 5 or 10 volume parts of P(S-*g*-EO). The volume compositions that were weighed out were based on the densities at room temperature. The density of the copolymer was estimated to be 1110 kg mol^{-3} by taking the weight-average values of PS (1060 kg m^{-3}) and PEO (1210 kg m^{-3}). Further details of the blending and sample preparation are presented elsewhere[24].

Instrumentation

Dynamic mechanical experiments were performed with a Rheometrics Dynamic Analyzer RDA II in the oscillatory mode. The solid-state samples with the shape of a rectangular parallelepiped had common approximate dimensions of $30 \times 12 \times 2$ mm^3, while the melt-state cylindrical samples had a diameter of 25 mm and an approximate thickness of 2 mm. The solid-state samples were subjected to a shear strain of a maximum of 0.1%, except for the PMMA/P(S-*g*-EO) 100/10 blend, which was subjected to a strain of 0.2%. The melt-state samples were subjected to a maximum strain of 10%. Angular frequency (ω) sweeps were performed from 500 to 0.02 rad s^{-1}, with a step size of up to ten points per decade. For the sake of simplicity, only the data at 0.02321 rad s^{-1} is presented in the text and figures, if nothing else is indicated. The samples were scanned at temperatures ranging from −80 to 250°C. The measurements were performed with different temperature steps over different temperature regions, but only the data at every 5°C is given in the figures. All measurements were performed by starting at a lower temperature and then increasing the temperature, with the exception of measurements in the temperature range from 25 to 150°C, which were performed by starting at 150°C and then decreasing the temperature. This procedure was adopted because the effect of any crystalline part of PEO in the blends should be eliminated in this temperature range which was above the onset of crystallization, i.e. at approximately 35°C in pure P(S-*g*-EO). The measurements were made by a Perkin-Elmer System 7 Differential Scanning Calorimeter by cooling pure P(S-*g*-EO) from 130°C at a rate of 5°C min^{-1}.

Scanning electron microscopy (SEM) studies were performed with a Zeiss DSM 920A instrument. Micrographs were taken on samples fractured in liquid nitrogen, and samples were taken both directly from the Brabender and from moulded d.m.s. samples. No difference in morphology between the two types of samples could be detected.

RESULTS AND DISCUSSION

Experimental observations

SEM pictures of two blends, i.e. PPO/PMMA (30/70) and PPO/PMMA/P(S-*g*-EO) (30/70/5), are shown in *Figure 2*. It can be observed that the addition of the copolymer reduces the size of the dispersed phase (PPO). This shows that the copolymer acts as a compatibilizer in the PPO/PMMA system, and indicates that at least a part of the copolymer is concentrated at the interphase between PPO and PMMA.

The experimental dynamic mechanical values of the dynamic shear storage modulus, $G'(\omega, T)$, and the dynamic shear loss modulus, $G''(\omega, T)$, for PPO, PMMA and P(S-*g*-EO) at temperatures in the range from 25 to 230°C ($\omega = 0.02\,321$ rad s^{-1}) are shown in *Figure 3*. In pure PPO, a glass transition with a maximum in G'' at 207°C ($\tan\delta$ maximum at 214°C) can be observed in the temperature range between 25 and 250°C. PMMA shows a distinct glass transition with a maximum in G'' at 100°C ($\tan\delta$ maximum at 108°C). Measurements of P(S-*g*-EO) show a maximum in G'' at −56°C ($\omega = 1$ rad s^{-1}), which corresponds to the glass transition of the amorphous PEO chains. To obtain data on P(S-*g*-EO) in the amorphous state in the temperature range of the calculations (25–250°C), measurements were also made from higher to lower temperatures, at temperatures at which the copolymer is completely amorphous (150–40°C). In this experiment, P(S-*g*-EO) shows much lower moduli values than PPO and PMMA. No maximum in G'' can be detected between 25 and 150°C, but a very small peak in $\tan\delta$ with a maximum at

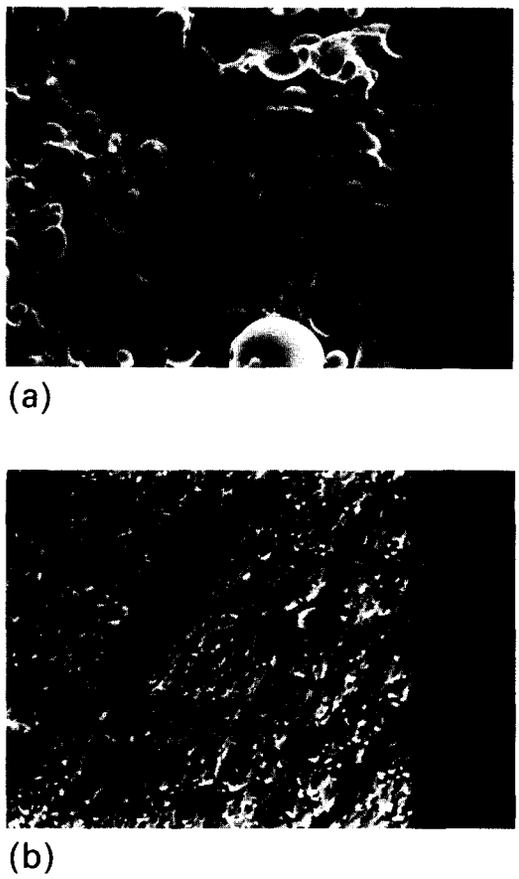

Figure 2 Scanning electron micrographs of fracture surfaces of (a) PPO/PMMA (30/70) and (b) PPO/PMMA/P(S-*g*-EO) (30/70/5) blends

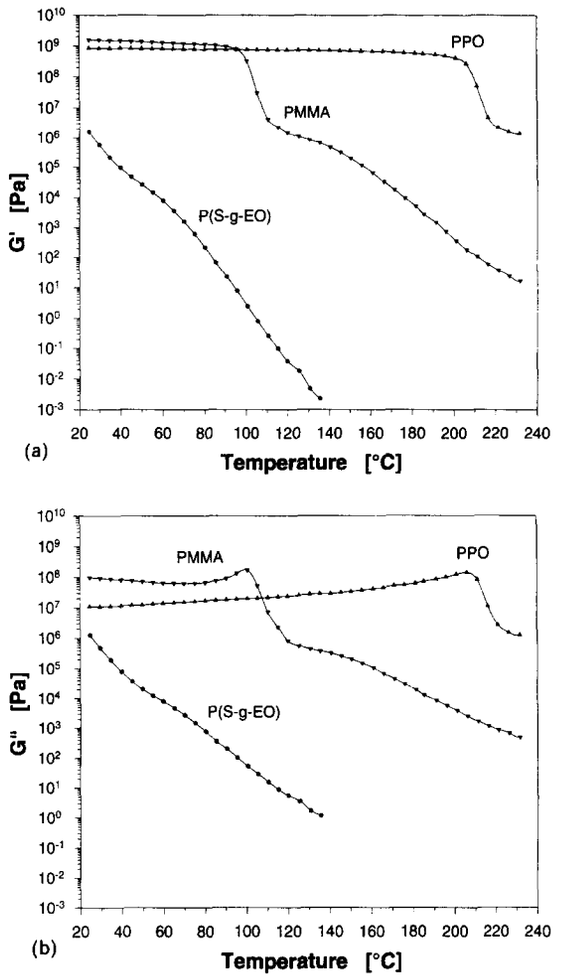

Figure 3 Experimental (a) $G'(\omega, T)$ and (b) $G''(\omega, T)$ values of PPO (▲), PMMA (▼) and P(S-*g*-EO) (●) in the temperature range from 25 to 230°C ($\omega = 0.02\,321$ rad s^{-1})

ca. 35°C is observable (determined by measurements made at higher temperatures and lower frequencies with the use of frequency–temperature superposition), after which tan δ rises sharply at higher temperatures.

Binary blends of P(S-*g*-EO) with each of the homopolymers also shows single T_g values in the temperature range from −80 to 250°C. PPO/P(S-*g*-EO) (100/10) has a maximum in G'' at 187°C (maximum in tan δ at 203°C), while PMMA/P(S-*g*-EO) has a maximum in G'' at 93°C (tan δ maximum at 105°C). This indicates that the interactions between one of the two components of the copolymer and each homopolymer are strong enough to make the two binary blends at least partially miscible. No crystallinity could be detected by d.m.s., differential scanning calorimetry (d.s.c.) or n.m.r. spectroscopy in these blends[24].

Figure 4 shows the experimental values of tan δ vs. temperature for the PPO/PMMA/P(S-*g*-EO) (30/70/Φ) system with different volume parts of P(S-*g*-EO) (Φ). The PPO/PMMA (30/70) blend shows a maximum in tan δ at ca. 111°C, corresponding to the glass transition of PMMA. Another transition corresponding to the glass transition of PPO can be discerned at ca. 212°C (not shown here). This behaviour, with two separate glass transitions, is typical for immiscible binary polymer blends. When P(S-*g*-EO) is added to the PPO/PMMA (30/70) blend, a new transition is observed at temperatures below 100°C. It can be observed in *Figure 4* that the position of the additional maximum in tan δ, as well as the peak size and shape, depend on the amount of copolymer added. When a

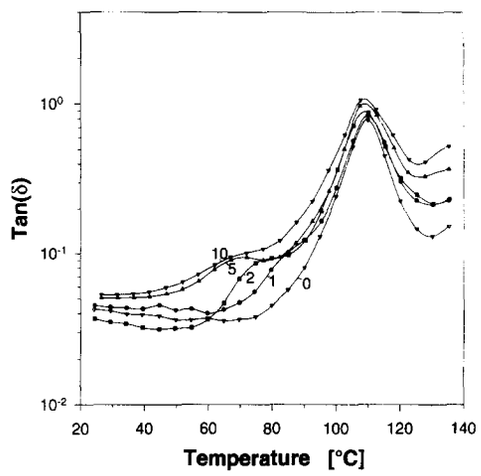

Figure 4 Experimental tan δ vs. temperature data for the PPO/PMMA/P(S-*g*-EO) (30/70/Φ) system, where Φ is 0 (▽), 1 (●), 2 (■), 5 (▲), and 10 (▼), in the temperature range from 25 to 135°C ($\omega = 0.02\,321$ rad s^{-1})

small amount of P(S-*g*-EO) is added, the new transition overlaps the glass transition of PMMA, but the additional peak shifts to lower temperatures and becomes further separated from the PMMA peak (which is shifted only a little) when the P(S-*g*-EO) content is increased. However,

the additional transition temperature is approximately constant when Φ is increased from 5 to 10 volume parts. The only difference between these two blends is a broadening of the PMMA transition towards lower temperatures for the 30/70/10 blend.

Micromechanical transitions

It can be observed from the experiments that no constituent has a distinct $\tan\delta$ maximum in the temperature region from 60 to 100°C. The additional transition of the PPO/PMMA/P(S-*g*-EO) system which is dependent on the amount of copolymer present can therefore not be explained by a molecular transition in any of the original materials. However, as both components of the copolymer are at least partially miscible with either PPO or PMMA, and as the SEM results show a great effect on the dispersed particle size with the addition of P(S-*g*-EO) to the PPO/PMMA blend, it is reasonable to assume that the copolymer is concentrated between the PPO and PMMA phases, i.e. that it forms a copolymer-rich interphase.

To demonstrate the origin and underlying mechanism of the additional transition in this complex heterogeneous material, we used the interlayer model to study the influence of a compatibilizer interphase on the viscoelastic properties of a theoretical blend. The properties of the matrix material ($|G^*_m| = 1.6$ GPa, $\delta_m = 0°$, $\nu_m = 0.5$) and the spherical particles ($|G^*_p| = 0.8$ GPa, $\delta_p = 0°$, $\nu_p = 0.5$) were chosen to be constant in these calculations, while the dynamic shear modulus of the interphase, $|G^*_i|$, was varied in the range from 1 to 10^7 Pa ($\delta_i = 45°$, $\nu_m = 0.5$). Calculations were performed for matrix/interphase/particle volume compositions of 70/0/30, 70/1/30, 70/2/30, 70/5/30 and 70/10/30. *Figure 5a* is a plot of the calculated quotient of the dynamic shear modulus of the blend and the matrix *versus* the dynamic shear modulus of the interphase. For each blend, the relative modulus shows a step between two values. The position of the modulus drop depends on the amount of interphase material and occurs at higher moduli values with increasing volume fractions of interphase. *Figure 5b* depicts the corresponding $\tan\delta$ values; it can be observed that the interlayer model predicts a maximum in $\tan\delta$, i.e. a transition, at a certain $|G^*_i|$ for the blend. The position of the $\tan\delta$ maximum obviously depends on the amount of interphase material in the same way as the position of the drop in modulus. Considering that the phase angles are constant for all the constituents, the existence of a transition in this matrix/interphase/particle system must originate from the change in the relative moduli of the constituents, as only the modulus of the interphase is changed. We have chosen to call this phenomenon a 'micromechanical transition' to distinguish it from ordinary molecular transitions. We will show below that micromechanical transitions can be observed experimentally in immiscible blends with an interphase, in good agreement with theoretical predictions.

Theoretical effect of an interphase in the PPO/PMMA/P(S-g-EO) system

By using the experimental $G'(\omega, T)$ and $G''(\omega, T)$ values at $\omega = 0.02321$ rad s^{-1} for PPO, PMMA and P(S-*g*-EO), we predict the resulting $G^*_b(\omega, T)$ values at various temperatures for different blends. Blends with

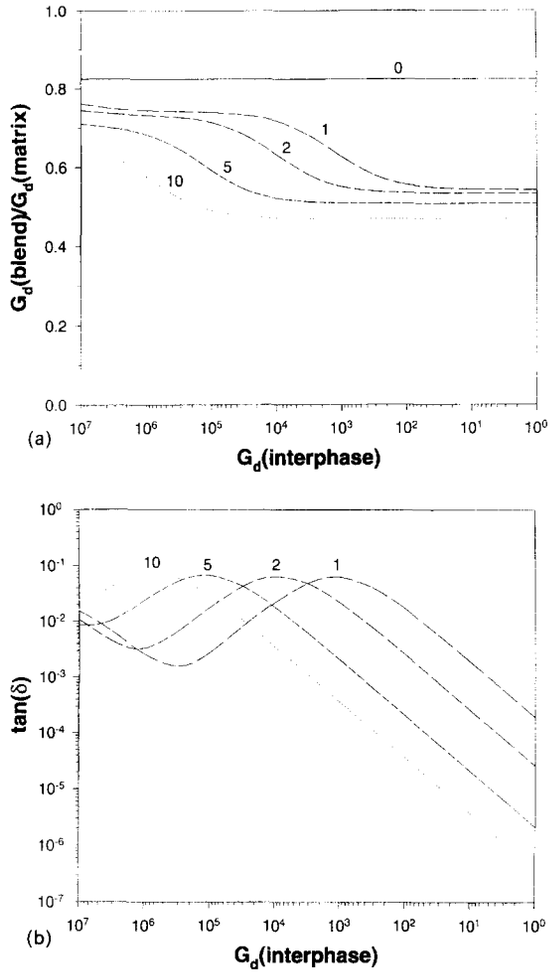

Figure 5 Theoretical modelling of a matrix/interphase/particle (70/Φ/30) blend, where Φ = 0, 1, 2, 5, and 10, as indicated on the figure: (a) $|G^*_b|/|G^*_m|$ vs. $|G^*_i|$; (b) $\tan\delta$ vs. $|G^*_i|$. Input data; for the matrix, $|G^*_m| = 1.6 \times 10^9$ Pa, $\delta_m = 0°$, $\nu_m = 0.5$, for the interphase, $|G^*_i|$ is variable, $\delta_i = 45°$, $\nu_i = 0.5$; for the particle phase, $|G^*_p| = 0.8 \times 10^9$ Pa, $\delta_p = 0°$, $\nu_p = 0.5$

the constant PPO/PMMA volume composition of 30/70 are studied, and it is assumed in all calculations that PPO forms spherical particles in a matrix of PMMA, if nothing else is indicated. This general assumption is reasonable according to the SEM results (see *Figure 2*).

To calculate the theoretical effect of an interphase in the PPO/PMMA/P(S-*g*-EO) (30/70/Φ) system, we utilized the original complex data of P(S-*g*-EO) as the input interphase data. In accordance with the experiments, the model predicts three transitions in the range from 25 to 250°C. Two of these predicted transitions, with $\tan\delta$ maxima at approximately 110 and 213°C, were expected and correspond to the glass transitions of PMMA and PPO, respectively. The former of these transitions can be observed in *Figure 6*, which presents the calculated values of $\tan\delta$ for the PPO/PMMA/P(S-*g*-EO) (30/70/Φ) system, with Φ ranging from 0 to 10 ($\nu_p = \nu_m = \nu_i = 0.5$), in the temperature range from 25 to 135°C. When $\Phi > 0$, a third loss maximum is predicted at temperatures below 100°C, which is shown for the different blends in *Figure 6*. This is in good agreement with experiments. The additional loss maximum cannot be explained by a transition in any of the original materials, as no constituent has a transition in this

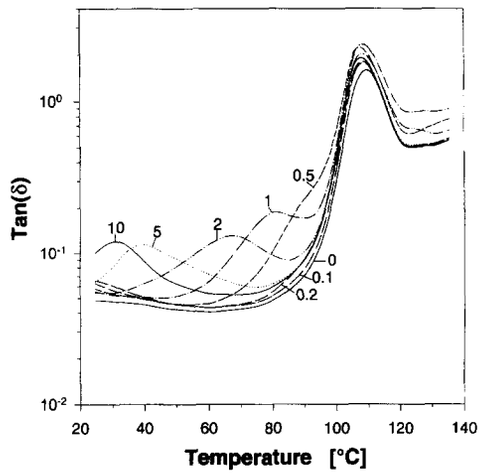

Figure 6 Theoretical values of tan δ at different temperatures between 25 and 135°C for the PPO/PMMA/P(S-*g*-EO) (30/70/Φ) system, where Φ is 0, 0.1, 0.2, 0.5, 1, 2, 5, and 10 ($\nu_m = \nu_p = \nu_i = 0.5$ and $\omega = 0.02321$ rad s^{-1})

temperature range (see *Figure 3*). However, the properties of the constituents of the PPO/PMMA/P(S-*g*-EO) system are similar to the properties of the matrix, interphase and particle phase in the theoretical blend described in *Figure 5*. The moduli of the matrix and the particle phase are approximately constant over the temperature range of the observed additional transition. On the other hand, the properties of the interphase change dramatically in this temperature range. It can therefore be concluded that the predicted additional transition in the ternary blends originates from the introduction of an interphase with certain specific characteristics, together with the relative moduli values of the matrix, interphase and particle phase.

As a comparison, we calculated the theoretical response of a PPO/PMMA/P(S-*g*-EO) (30/70/2) blend by assuming that the copolymer would form spherical particles in the PPO phase. In other words, we assumed that PMMA would continue to be the matrix, the copolymer would form the particles and PPO would form a thick interphase around the copolymer particles. In this case, the effect of the copolymer phase was negligible, and no additional transition was predicted. Further calculations, using the assumptions of different constant values of $G_i'(\omega, T)$ ($G_i''(\omega, T) = 0$) or different constant values of $G_i' = G_i''$ for all temperatures, also predicted an effect on the response of the blend, but a maximum in tan δ could not be predicted. This clearly shows that certain interphase conditions are necessary to obtain a micromechanical transition in a blend.

In comparison with the experiments, the theoretical maximum value of tan δ for the PMMA peak is higher than the experimental value. According to previous work[22], a reason for this may be that the particle phase does not form perfectly spherical particles in the matrix. Instead, it is more likely that most of the particles are more or less extended and that some particles agglomerate, giving some form of continuity of the particle phase, which results in more of the material being elastic. This is also verified by the G' vs. temperature data of these blends, where the experimental shear storage modulus does not decrease as much as the theoretical calculations predict at temperatures between the glass transitions of PMMA and PPO.

Theoretical effect of the volume fraction of the interphase

In *Figure 6*, it can be observed that the micromechanical transition temperature is predicted to depend on the total volume fraction of the interphase, i.e. on the amount of added copolymer. At low volume fractions of the interphase, the additional peak is predicted to overlap the PMMA peak. With an increasing amount of interphase material, the additional peak is shifted to lower temperatures and thus becomes further separated from the PMMA peak. The calculations show that the dependence of the micromechanical transition temperature on the total volume fraction of the interphase is greatest for small quantities of interphase material. The qualitative behaviour of these predictions is in good agreement with the experiments.

It should be noted that the interlayer model is independent of the spherical particle size. A certain amount of interphase will give a certain quotient between the volume fraction of the interphase and the spherical particles, i.e. the relation between the distances a and b in *Figure 1a* are independent of the spherical particle size and spherical particle size distribution and depend only on the total volume fractions, according to equation (2). This means that the theoretical response for a blend with small particles and thin interphases will be the same as that for a blend with large particles and thick interphases, as long as the volume fractions of the particles and interphase are constant. Although the particle size is less than 1 μm in some blends, the effect of the interfacial tension is still negligible as we have been studying blends in the solid state. Thus, the observed reduction in particle size with the addition of copolymer does not affect the basic theoretical modelling.

It can be observed both from experiments and theory that the additional tan δ peak is large in relation to the size of the PMMA peak, taking into account in the calculations that the amount of the PMMA phase is 7–700 times larger than the P(S-*g*-EO) phase. We conclude that the size of the tan δ peak for micromechanical transitions is not very dependent on the total volume of the interphase. It can instead be shown that the size is governed by the specific levels of the moduli and phase angles of the constituents.

There are other phenomena that may hypothetically give rise to an additional tan δ maximum. Crystallinity and melting may affect the viscoelastic response of the blends; however, although the PEO side chains are at least partially crystalline in the pure copolymer, previous experiments[24] could not detect any melt peak in the d.s.c. measurements, or any crystalline part in the n.m.r. spectroscopic measurements, for any of the binary (PPO/P(S-*g*-EO) (100/10) and PMMA/P(S-*g*-EO) (100/10) or ternary (PPO/PMMA/P(S-*g*-EO) (30/70/Φ) blends. If there is still a small amount of PEO that can crystallize at lower temperatures, the experimental procedure, with frequency scans starting at higher and ending at lower temperatures, prevents the PEO from becoming crystalline at temperatures in the range of the additional tan δ maximum. The additional transition is therefore not considered as being caused by melting or crystallization of PEO in the blends. The dependence of the transition temperature on the amount of added copolymer, with a tan δ maximum in our blends at temperatures

between 60 and 100°C (which is lower than for pure PS, PMMA and PPO), could also be explained by the existence of a third phase in the blends, in which the PEO part of the copolymer is mixed with PMMA (not an interphase). This could theoretically give transitions in this temperature range, but we would then expect the PMMA peak to be smaller, as the only change in morphology is that the particles become smaller when the copolymer is added. However, the PMMA peak in the ternary blends is as large as or larger than the PMMA peak in the PPO/PMMA (30/70) blend, and thus this is not a good explanation for the existence of the additional transition. In conclusion, the theory strongly indicates that the experimentally observed loss peak in the ternary blends is a micromechanical transition, which is caused by the introduction of an interphase with certain specific properties.

Theoretical effect of horizontal and vertical shifts of the original P(S-g-EO) data

Compared with the experimental tan δ values of the PPO/PMMA/P(S-*g*-EO) (30/70/Φ) blends, the theory predicts lower micromechanical transition temperatures for each composition when using the original P(S-*g*-EO) data for the interphase. When an interphase is created by the addition of a copolymer, it is reasonable to assume that the interphase is diffuse and that it contains not only the copolymer, but also homopolymer chains with different concentration profiles, particularly if the copolymer is miscible with the homopolymers. The mixing should thus give an interphase material that is influenced by the properties of PPO and PMMA[24], giving a higher modulus and a more elastic component when compared with the original copolymer data, according to the original complex data in *Figure 3*. In addition to the volume fraction of the interphase being affected by this, it is possible to state in a qualitative discussion that the actual average complex properties of the interphase are shifted in the horizontal direction towards higher temperatures and/or in the vertical direction towards higher moduli values, in comparison with the original copolymer data. With these assumptions, it is relevant to shift the original complex P(S-*g*-EO) data in the horizontal or vertical directions, and to use the shifted data as the interphase properties in order to study the qualitative effect of the influence of PPO and PMMA on the interphase, and to compare the theoretical response with the experimental results.

The horizontal shifting of P(S-*g*-EO) was performed by shifting the original complex data, i.e. both $G_d(\omega, T)$ and $\delta(\omega, T)$ of P(S-g-EO), along the temperature axis to higher temperatures in steps of 5, 10, 15 and 20°C, before the material data (denoted as P(S-*g*-EO)*) for the interphase were introduced into the calculations. The effect of the horizontal shifting is presented for the PPO/PMMA/P(S-*g*-EO)* (30/70/1) blend in *Figure 7a*. The step in the horizontal shift for each calculation is indicated on the figure (the solid line represents the calculations using the original P(S-*g*-EO) data). It is observed that the position of the micromechanical transition is also shifted to higher temperatures, with approximately the same step as the shifted copolymer data. The size and appearance of the peaks are changed only very slightly by this operation. It can also be observed that the shifting of the original P(S-*g*-EO) data

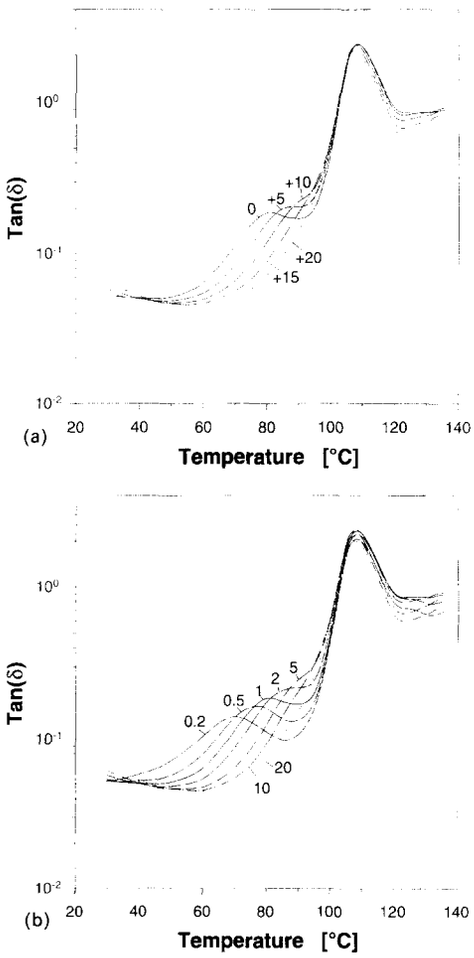

Figure 7 Theoretical values of tan δ at different temperatures between 25 and 135°C for different blends: (a) the PPO/PMMA/P(S-*g*-EO)* (30/70/1) blend, for which the original G' and G'' vs. temperature data of P(S-*g*-EO) have been shifted horizontally by 0, 5, 10, 15, and 20°C along the temperature axis towards higher temperatures; (b) the PPO/PMMA/P(S-*g*-EO)** (30/70/1) blend, for which the original G' and G'' vs. temperature data of P(S-*g*-EO) have been shifted vertically along the modulus axis by multiplying the original data by a factor of 0.2, 0.5, 1, 2, 5, 10 and 20, as noted on the figure ($\nu_m = \nu_p = \nu_i = 0.5$ and $\omega = 0.02321$ rad s^{-1})

by 10°C to higher temperatures results in a response that is quantitatively similar to the actual experimental response of the corresponding blend.

We also studied the effect of shifting the original $G_d(\omega, T)$ data of P(S-*g*-EO) vertically along the modulus axis, without changing the $\delta(\omega, T)$ values (the vertically shifted data are denoted as P(S-*g*-EO)**). The effect of this operation is shown in *Figure 7b* for the PPO/PMMA/P(S-*g*-EO)** (30/70/1) blend. The values next to the curves in the figure correspond to the factor which was multiplied with the original $G_d(\omega, T)$ data of P(S-*g*-EO) before these data were used in the calculations. We observe that an increasing modulus of the interphase has the same effect as shifting the $G_d(\omega, T)$ and $\delta(\omega, T)$ values horizontally towards higher temperatures, and that a vertical $G_d(\omega, T)$ shift by a factor of five results in approximately the same response as a horizontal shift of the complex data by a step of 10°C.

Theoretical effect of the Poisson ratio of the matrix, interphase and particle phase

The theoretical effect of the Poisson ratios of the

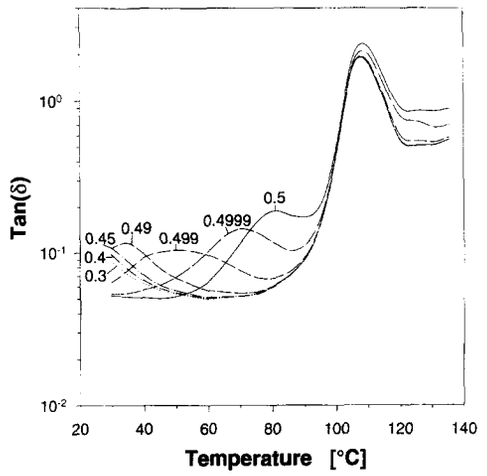

Figure 8 Theoretical effect of different Poisson ratios for the interphase ($\nu_i = 0.3$–0.5) on the tan δ values of the PPO/PMMA/P(S-*g*-EO) (30/70/1) blend at temperatures ranging from 25 to 135°C ($\nu_m = \nu_p = 0.5$ and $\omega = 0.02321$ rad s^{-1})

matrix (ν_m), particles (ν_p) and interphase (ν_i) on the viscoelastic response is quite different, with ν_m and ν_p affecting the viscoelastic response (tan δ) of the PPO/PMMA/P(S-*g*-EO) system only marginally. A small increase in tan δ is detected in the temperature range of the micromechanical transition as ν_m is decreased from 0.5 to 0.3 ($\nu_i = \nu_p = 0.5$), while a similar decrease in ν_p ($\nu_m = \nu_i = 0.5$) results only in a very small decrease in tan δ in the same temperature range. We therefore conclude that the compressibility of the matrix and the particle phase has only a limited effect on the viscoelastic response of this blend between 25 and 135°C. On the other hand, ν_i is predicted to affect the viscoelastic response of the PPO/PMMA/P(S-*g*-EO) (30/70/1) blend dramatically, as shown in *Figure 8* ($\nu_m = \nu_p = 0.5$). We observe that the position of the micromechanical transition is shifted ca. 50°C towards lower temperatures when ν_i goes from 0.5 to 0.49. The dependence of ν_i is greater the closer it is to 0.5, and when ν_i has a value of less than 0.45, the effect of a further decrease of ν_i has only a small effect on the theoretical response. This is a strong indication that the compressibility of the interphase in a polymer blend may substantially affect the viscoelastic response of the blend.

CONCLUSIONS

It has been shown that the dispersed particle size in the PPO/PMMA/P(S-*g*-EO) system is decreased by the addition of the graft copolymer, which demonstrates that the copolymer acts as a compatibilizer in this system. Dynamic mechanical experiments show that a small addition (1–10 volume parts) of P(S-*g*-EO) to a PPO/PMMA (30/70) blend results in a new transition in the ternary blend. The position of this transition was found at temperatures ranging from 60 to 100°C, depending on the amount of P(S-*g*-EO) added (the transition temperature decreased when the amount of copolymer was increased).

By using an interlayer model for the ternary blends, which assumes that spherical PPO particles, covered by a shell of P(S-*g*-EO) (interphase), are formed in a PMMA matrix, it was possible to predict the dynamic mechanical behaviour of the blends. The existence of the additional transition found in the experimental ternary PPO/PMMA/P(S-*g*-EO) blends was also predicted in the same temperature range by the theory. It should be noted that only the original complex moduli, the volume fractions and the Poisson ratios of the constituents were introduced in the model. This means that the interlayer model predicts a transition in the ternary blends at a position at which no constituent has a transition. This phenomenon was called micromechanical transition to distinguish it from ordinary molecular transitions, and was explained by the change in relative values of the moduli of the components in the matrix–interphase–particle structure of the blends.

The agreement between experiment and theory on the micromechanical transition in the PPO/PMMA/P(S-*g*-EO) system is a strong indication of the true existence of an interphase with its own characteristic properties. The dependence of the position of the micromechanical transition on the volume fraction of the added copolymer is also verified theoretically, and the theory also predicts a strong dependence on the Poisson ratio of the interphase.

It can be concluded from these calculations that the existence, position and size of a micromechanical transition are directly dependent on the viscoelastic data of the interphase, matrix and particle phase, and that its existence does not require any particular transition in the interphase itself. Our calculations thus show that an interphase can have a strong effect on the viscoelastic response of a polymer blend, and that interphases may cause micromechanical transitions in blends, independent of whether the interphase itself has a transition.

ACKNOWLEDGEMENTS

We gratefully acknowledge the National Swedish Board For Industrial and Technical Development (NUTEK) for their financial support of this work. We also thank Patric Jannasch for the preparation and characterization of the graft copolymer and Anders Mårtensson for providing the SEM pictures.

REFERENCES

1 Teyssié, Ph., Fayt, R. and Jerome, R. *Makromol. Chem. Macromol. Symp.* 1988, **16**, 41
2 van Ballegooie, P. and Rudin, A. *Makromol. Chem.* 1989, **90**, 3153
3 Heuschen, J., Vion, J. M., Jerome, R. and Teyssié, Ph. *Polymer* 1990, **31**, 1473
4 Thomas, S. and Prud'homme, R. E. *Polymer* 1992, **33**, 4260
5 Perrin, P. and Prud'homme, R. E. *Macromolecules* 1994, **27**, 1852
6 Tang, T. and Huang, B. *Polymer* 1994, **35**, 281
7 Maurer, F. H. J. in 'Polymer Composites' (Ed. B. Sedlacek), Walter de Gruyer, Berlin, 1986, p. 399
8 Maurer, F. H. J. in 'Controlled Interphases in Composite Materials' (Ed. H. Ishida), Elsevier, New York, 1990, pp. 491–504
9 van der Poel, C. *Rheol. Acta* 1958, **1**, 198
10 Schwarzl, F. R. and van der Eikhoff, J. 'Calculation of Elastic Properties of Composites by Means of the van der Poel Theory', Central Laboratory TNO Delft, The Netherlands, Report No. CL 71/55, 1971
11 Smith, J. C. *J.Res. Natl. Bur. Stand. Sect.* 1974, **78A**, 355

12 Maurer, F. H. J., Papazoglu, E. and Simha, R. in 'Advanced Concepts of Interfaces in Polymer Ceramic and Metal Matrix Composites 2' (Ed. H. Ishida), Elsevier, Amsterdam, 1988, p. 747
13 Papazoglu, E., Simha, R. and Maurer, F. H. J. *Rheol. Acta* 1989, **28**, 302
14 Steeman, P. A. M. and Maurer, F. H. J. *Colloid Polym. Sci.* 1990, **268**, 315
15 Steeman, P. A. M and Maurer, F. H. J. *Colloid Polym. Sci.* 1992, **270**, 1069
16 Palierne, J. F. *Rheol. Acta* 1990, **29**, 204
17 Graebling, D., Muller, R. and Palierne, J. F. *Macromolecules* 1993, **26**, 320
18 Greabling, D., Benkira, A., Gallot, Y. and Muller, R. *Eur. Polym. J.* 1994, **30**, 301
19 Germain, Y., Ernst, B., Genelot, O. and Dhamani, L. *J. Rheol.* 1994, **38**, 681
20 Gramespracher, H. and Meissner, J. *J. Rheol.* 1992, **26**, 1127
21 Schwarzl, F. R. *Acta Phys. Austriace Bnd* 1965, **22**, 15
22 Eklind, H. and Maurer, F. H. J. *Polym. Networks Blends* 1995, **5**, 35
23 Brown, H. R., Char, K. and Deline, V. R. *Macromolecules* 1993, **26**, 4164
24 Eklind, H., Schantz, S., Maurer, F. H. J., Jannasch, P. and Wesslén, B. *Macromolecules* 1996, **29**, 984.
25 Eklind, H. and Maurer, F. H. J. *J. Polym. Sci. Polym. Phys. Edn* in press
26 Maurer, F. H. J. *PhD Thesis*, University of Duisberg, 1983
27 Einstein, A. *Ann. Physik* 1911, **34**, 591
28 Christensen, R. S. 'Mechanics of Composite Materials', Wiley, New York, 1979
29 Jannasch, P. and Wesslén, B. *J. Polym. Sci. Polym. Chem. Edn* 1993, **31**, 1519

APPENDIX

The elements of $|\alpha|$, $|\beta|$, $|\gamma|$ and $|\tau|$ which are not specified below have the value of zero.

The elements of the subdeterminant $|\alpha|$

$$M = \frac{G_p^*(\omega, T)}{G_i^*(\omega, T)}$$

$$P = \frac{G_i^*(\omega, T)}{G_m^*(\omega, T)}$$

$$\alpha[1,1] = \alpha[2,1] = M$$

$$\alpha[1,2] = -\tfrac{1}{2} M \Phi_p^{2/3}$$

$$\alpha[1,3] = -1$$

$$\alpha[1,4] = 4\Phi_p^{-5/3}$$

$$\alpha[1,5] = \tfrac{1}{2}\Phi_p^{2/3}$$

$$\alpha[1,6] = \Phi_p^{-1}\frac{(10-2\nu_i)}{(5-4\nu_i)}$$

$$\alpha[2,2] = M\Phi_p^{2/3}\frac{(7+2\nu_p)}{6\nu_p}$$

$$\alpha[2,3] = -1$$

$$\alpha[2,4] = -\tfrac{8}{3}\Phi_p^{-5/3}$$

$$\alpha[2,5] = -\Phi_p^{2/3}\frac{(7+2\nu_i)}{6\nu_i}$$

$$\alpha[2,6] = -\Phi_p^{-1}\frac{(2+2\nu_i)}{(5-4\nu_i)}$$

$$\alpha[3,1] = \Phi_p^{1/3}$$

$$\alpha[3,2] = \Phi_p$$

$$\alpha[3,3] = -\Phi_p^{1/3}$$

$$\alpha[3,4] = -\Phi_p^{4/3}$$

$$\alpha[3,5] = -\Phi_p$$

$$\alpha[3,6] = -\Phi_p^{-2/3}$$

$$\alpha[4,1] = \tfrac{1}{2}\Phi_p^{1/3}$$

$$\alpha[4,2] = \Phi_p\frac{(7-4\nu_p)}{12\nu_p}$$

$$\alpha[4,3] = -\tfrac{1}{2}\Phi_p^{1/3}$$

$$\alpha[4,4] = \tfrac{1}{3}\Phi_p^{-4/3}$$

$$\alpha[4,5] = -\Phi_p\frac{(7-4\nu_i)}{12\nu_i}$$

$$\alpha[4,6] = -\Phi_p^{-2/3}\frac{(1-2\nu_i)}{(5-4\nu_i)}$$

$$\alpha[5,3] = P$$

$$\alpha[5,4] = -4P(\Phi_p+\Phi_i)^{-5/3}$$

$$\alpha[5,5] = -\tfrac{1}{2}P(\Phi_p+\Phi_i)^{2/3}$$

$$\alpha[5,6] = -P(\Phi_p+\Phi_i)^{-1}\frac{(10-2\nu_i)}{(5-4\nu_i)}$$

$$\alpha[5,7] = -1$$

$$\alpha[5,8] = 4(\Phi_p+\Phi_i)^{-5/3}$$

$$\alpha[5,9] = \tfrac{1}{2}(\Phi_p+\Phi_i)^{2/3}$$

$$\alpha[5,10] = (\Phi_p+\Phi_i)^{-1}\frac{(10-2\nu_m)}{(5-4\nu_m)}$$

$$\alpha[6,3] = P$$

$$\alpha[6,4] = \tfrac{8}{3}P(\Phi_p+\Phi_i)^{-5/3}$$

$$\alpha[6,5] = (\Phi_p+\Phi_i)^{2/3}P\frac{(7+2\nu_i)}{6\nu_i}$$

$$\alpha[6,6] = (\Phi_p+\Phi_i)^{-1}P\frac{(2+2\nu_i)}{(5-4\nu_i)}$$

$$\alpha[6,7] = -1$$

$$\alpha[6,8] = -\tfrac{8}{3}(\Phi_p+\Phi_i)^{-5/3}$$

$$\alpha[6,9] = -(\Phi_p+\Phi_i)^{2/3}\frac{(7+2\nu_m)}{6\nu_m}$$

$$\alpha[6,10] = -(\Phi_p+\Phi_i)^{-1}\frac{(2+2\nu_m)}{(5-4\nu_m)}$$

$$\alpha[7,3] = (\Phi_p+\Phi_i)^{1/3}$$

$$\alpha[7,4] = (\Phi_p+\Phi_i)^{-4/3}$$

$$\alpha[7,5] = \Phi_p+\Phi_i$$

$$\alpha[7,6] = (\Phi_p+\Phi_i)^{-2/3}$$

$$\alpha[7,7] = -(\Phi_p+\Phi_i)^{1/3}$$

$$\alpha[7,8] = -(\Phi_p + \Phi_i)^{-4/3}$$

$$\alpha[7,9] = -(\Phi_p + \Phi_i)$$

$$\alpha[7,10] = -(\Phi_p + \Phi_i)^{-2/3}$$

$$\alpha[8,3] = \tfrac{1}{2}(\Phi_p + \Phi_i)^{1/3}$$

$$\alpha[8,4] = -\tfrac{1}{3}(\Phi_p + \Phi_i) - 4/3$$

$$\alpha[8,5] = (\Phi_p + \Phi_i)\frac{(7 - 4\nu_i)}{12\nu_i}$$

$$\alpha[8,6] = (\Phi_p + \Phi_i)^{-2/3}\frac{(1 - 2\nu_i)}{(5 - 4\nu_i)}$$

$$\alpha[8,7] = -\tfrac{1}{2}(\Phi_p + \Phi_i)^{1/3}$$

$$\alpha[8,8] = -\tfrac{1}{3}(\Phi_p + \Phi_i)^{-4/3}$$

$$\alpha[8,9] = -(\Phi_p + \Phi_i)\frac{(7 - 4\nu_m)}{12\nu_m}$$

$$\alpha[8,10] = --(\Phi_p + \Phi_i)^{-2/3}\frac{(1 - 2\nu_m)}{(5 - 4\nu_m)}$$

$$\alpha[9,7] = \tfrac{5}{2}$$

$$\alpha[9,9] = 1 + 3\frac{(7 - 4\nu_m)}{12\nu_m}$$

$$\alpha[9,10] = 1 + 3\frac{(1 - 2\nu_m)}{(5 - 4\nu_m)}$$

$$\alpha[10,7] = \tfrac{1}{2}$$

$$\alpha[10,8] = -\tfrac{1}{3}$$

$$\alpha[10,9] = \frac{(7 - 4\nu_m)}{12\nu_m}$$

$$\alpha[10,10] = \frac{(1 - 2\nu_m)}{(5 - 4\nu_m)}$$

The elements of the subdeterminant $|\beta|$

$$\beta[9,7] = 0$$

$$\beta[9,8] = -\frac{20}{3}$$

$$\beta[9,9] = -\tfrac{1}{2} - \frac{(7 + 2\nu_m)}{6\nu_m}$$

$$\beta[9,10] = -\frac{(10 - 2\nu_m)}{(5 - 4\nu_m)} - \frac{(2 + 2\nu_m)}{(5 - 4\nu_m)}$$

$$\beta[10,7] = \tfrac{5}{2}$$

$$\beta[10,8] = 0$$

$$\beta[10,9] = 1 + 3\frac{(7 - 4\nu_m)}{12\nu_m}$$

$$\beta[10,10] = 1 + 3\frac{(1 - 2\nu_m)}{(5 - 4\nu_m)}$$

The elements of the subdeterminant $|\gamma|$

$$\gamma[9,9] = -\tfrac{1}{2} + \tfrac{3}{2}\frac{(7 + 2\nu_m)}{6\nu_m}$$

$$\gamma[9,10] = -\frac{(10 - 2\nu_m)}{(5 - 4\nu_m)}$$

$$\gamma[10,7] = 0$$

$$\gamma[10,8] = \tfrac{5}{3}$$

$$\gamma[10,9] = 1 - 2\frac{(7 - 4\nu_m)}{12\nu_m}$$

$$\gamma[10,10] = 1 - 2\frac{(1 - 2\nu_m)}{(5 - 4\nu_m)}$$

The elements of the subdeterminant $|\tau|$

$$\tau[9,9] = -\tfrac{1}{2} + \tfrac{3}{2}\frac{(7 + 2\nu_m)}{6\nu_m}$$

$$\tau[9,10] = -\frac{(10 - 2\nu_m)}{(5 - 4\nu_m)} + \frac{3}{2}\frac{(2 + 2\nu_m)}{(5 - 4\nu_m)}$$

$$\tau[10,7] = 1$$

$$\tau[10,8] = \tfrac{8}{3}$$

$$\tau[10,9] = \frac{(7 + 2\nu_m)}{6\nu_m}$$

$$\tau[10,10] = \frac{(2 + 2\nu_m)}{(5 - 4\nu_m)}$$